

## SCOUR DOWNSTREAM OBLIQUE V-NOTCH WEIR

Y. A. Hamed, M. H. El-Kiki and A. M. Mirdan

Civil Engineering Department, Faculty of Engineering, Suez Canal University  
Port Fouad - Port Said, Egypt  
E-mail: [Yasser\\_ham@hotmail.com](mailto:Yasser_ham@hotmail.com)

### ABSTRACT

Scour in bed material downstream weirs is considered the most unfavorable process which threatens the overall stability of the weir. Weirs with oblique angle in the horizontal plan will affect the scour profile downstream the structure and may reduce it. The objective of this paper is to investigate the effect of oblique weir angle on the scour profile. Furthermore, the effect of V-notch angle on the scour profile will be studied. In order to achieve that, laboratory experiments were carried out to test four weirs models of different V-notch angle 30°, 60°, 90° and 120°. Experiments were conducted at three different Froude numbers and four different oblique angles of the weir (0 (normal to the flow), 5, 10 and 15°). The results showed that scour parameters (maximum scour depth and volume of scour) can be decreased by placing the V-notch weir with small oblique angle. The changes in scour parameters for V-notch angles 30, 60 and 90 were not significant while it decreased significantly by using 120° weir. By increasing oblique weir angle, maximum scour depth/length will be increased significantly adjacent to one of the walls. Higher oblique angles will cause the flow to hit the channels sides and affect the structure walls. Empirical equations defining maximum scour depth/length and scour hole with different variables were developed.

**Keywords:** Scour, V-notch weir, Oblique, Open channel

### INTRODUCTION

The characteristics and hydraulic behavior of plain weirs or standard weirs have been studied for a long time and the understanding on them is rather deep. However, few studies have been done on weirs placed obliquely in the flow.

Borghai et al. (2003) [6] published their study on the discharge coefficient for oblique rectangular sharp-crested weir. Their research demonstrated the influence of the oblique angle to the discharge coefficient  $C_d$  resulting in a single formula for  $C_d$ , and correction coefficients for submerged flow. Prakash and Shivapur (2004) [12] studied flow over an oblique V-notch weir. Based on experimental work on 0° (normal) and 15, 30, 45, and 60° weirs, they have established an equation for discharge in terms of the oblique angle of the weir plane with the plane normal to the flow axis. Tuyen (2006) [14] conducted a laboratory investigation on the flow over different types of

oblique weirs (rectangular sharp-crested weir, a rectangular broad-crested weir) including behavior and hydraulic characteristic of the flow, different phenomena in the neighborhood of the weir, and hydraulic parameters and physical laws that govern the process. He concluded that by increasing the oblique angle, the effective length of the weir increases significantly, whereas the discharge coefficient  $C_d$  slightly decreases. Together they make the discharge capacity of the oblique weir increases.

Scour process is caused by sediment transportation resulted from the flow of the fluid. When the sediment rate transported into a certain area is less than that transported out of this area, a scour hole will be existed. Local scour is caused by local disturbance in the flow such as vortices and eddies. These disturbances are due to obstructions affecting the stream flow. Local scour causes the lowering of a defined small portion of the channel bed below its natural level. In case of hydraulic control structures, i.e. weirs, the scour process affects the downstream reach. This is owing to the turbuncy results while changing of flow state from supercritical to subcritical flow downstream these structures.

Ashour et al. (2008) [5], studied scour downstream curved weirs and compared it with that downstream straight ones. They used five models of weirs having different crest length and different downstream face. They found a certain arrangement of a curved weir together with two groups of sills located on the solid apron which gave minimum scour profile. Based on the examination of topography of scour hole produced by different hydraulic conditions, many researchers studied local scour of alluvial channel near rigid apron (i.e. Abo-Zeid (2004) [1], (2006) [2]; Ali (1996) [4]; Hassan et al. (1986) [7]; Hemaïd (2000) [8]; Kamil (2002) [9]; Negm et al. (2002) [11]; Roudkivi et al. (1983) [13]; Youssef (2004) [15]). Ali (1995) [3] concluded that the use of end sills may increase the scour behind the regulators. He found that the suitable location of the baffle sills depend on the sill height and tail water depth. Nasr and Nagy (1997) [10] studied theoretically scour downstream spillway and they managed to develop a theoretical formula for estimating scour hole depth.

The main objective of this paper is to investigate the effect of oblique V-notch weir on the scour profile downstream the structure. Furthermore, the effect of both of different V-notch angle and different Froude numbers on the scour profile will be studied

## **DIMENSIONAL ANALYSIS**

The dimensional analysis was carried out to derive an expression for the scour parameters ( $d_s$ : depth of scour hole,  $L_s$ : Length of scour hole and  $V_s$ : volume of scour hole (Figure (1)). The rest of the variables considered are;  $d_{50}$ : mean particle diameter,  $g$ : gravitational acceleration,  $\theta$ : V-notch angle,  $\alpha$ : oblique angle of the weir in the horizontal plan,  $V$ : normal mean velocity at the downstream cross section of the channel,  $H$ : working head of the weir,  $H_d$ : downstream water depth,  $\gamma_w$ : specific weight of water,  $\gamma_s$ : soil particle specific weight,  $\nu$ : kinematic viscosity,  $t$ : time of the run.

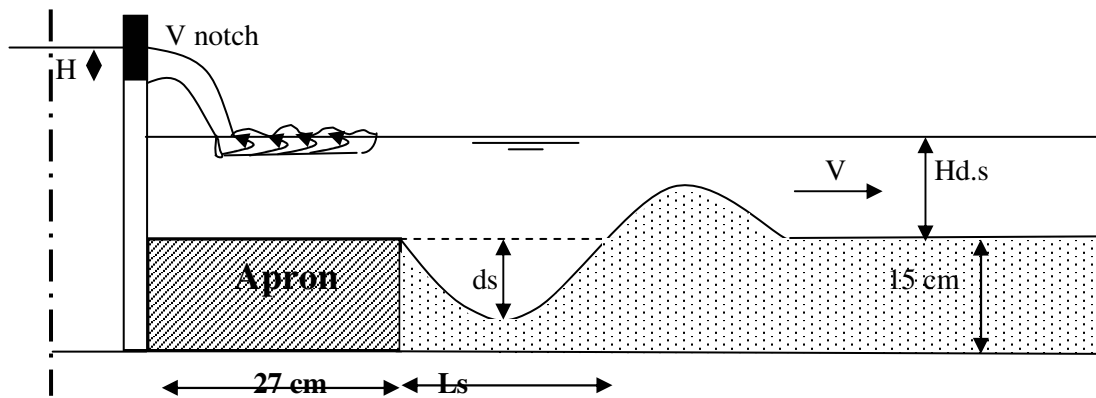


**Fig. (1) Schematic diagram showing the geometry of the scour hole and the flow parameters**

The scour parameters may depend upon the other remaining parameters as follow:

$$ds \text{ or } Ls \text{ or } Vs = \varphi_1 ( Hd.s, H, \alpha, \theta, V, d_{50}, g, \gamma_s, \gamma_w, u, t ) \tag{1}$$

Using  $\pi$ -Theory, the following can be concluded:

$$\frac{ds}{Hd.s} \text{ or } \frac{Ls}{Hd.s} \text{ or } \frac{Vs}{(Hd.s)^3} = \varphi_2 \left( \frac{H}{Hd.s}, \frac{\gamma_w}{\gamma_s}, \frac{V}{\sqrt{gHd.s}}, \frac{v}{VHd.s}, \frac{d_{50}}{Hd.s}, \frac{V.t}{Hd.s}, \alpha, \theta \right) \tag{2}$$

in which  $V/\sqrt{gHd.s}$ = Froude number (Fr) and  $v/VHd.s = 1/\text{Reynolds number (Re)}$

Fluid viscosity has a smaller effect in which Re can be neglected. The head effect (H) may be considered in the variables Fr while  $d_{50}$ ,  $\gamma_s$  and  $t$  were kept constant during the experiments, consequently Eq (2) can be reduced to:

$$\frac{ds}{Hd.s} \text{ or } \frac{Ls}{Hd.s} \text{ or } \frac{Vs}{(Hd.s)^3} = \varphi_3 (Fr, \alpha, \theta) \tag{3}$$

## METHODS AND MATERIALS

The experimental work of this study was conducted at the hydraulic laboratory of Faculty of Engineering, Suez Canal University during the period from the first of August to the end of October 2008.

**Flume:** A re-circulating rectangular flume was used (Figure (2)). It is a closed operating system with an overall length of 13.25 m. It consists of three parts, the inlet, the testing part and the outlet of lengths 1.7 m, 10 m and 1.375 m respectively. The inlet part of the flume has a depth of 105 cm and width of 50 cm and made from fiber glass. A feeding pipe from the pump gives the inlet part its capacity of water. The

testing part of the flume has a depth of 50 cm and width of 30 cm. The vertical sides of the flume are made from glass of thickness 1.2 cm while its bed is made of a cold rolled steel sheets welded to each other. The outlet part has a depth of 68 cm and width of 30 cm and made of fiber glass. A pipe of 20 cm diameter is attached to the outlet part and working as an exit for the flume. The flow rates were measured by a pre-calibrated 90° V-notch which using the following empirical formula deduced from calibration:

$$Q = 1.474 H^{2.5} \quad (4)$$

where Q: the discharge in m<sup>3</sup>/sec, H: the head over the crest in m.

Water depths and bed levels were measured by a point gauge. A solid apron of distance 27 cm was placed downstream the weir models. The apron length was checked by Bligh formula of the scour length:

$$L = 0.61 C_B H_s^{0.5} \quad (5)$$

where  $H_s$ : the difference between upstream water level and critical depth ( $\sqrt[3]{q^2/g}$ ) where q: discharge per unit width of the flume.

The apron was followed by 6 m long of mobile bed which has  $d_{50}=0.76\text{mm}$  and thickness of 15 cm. Both of the apron and the sand have the same level.

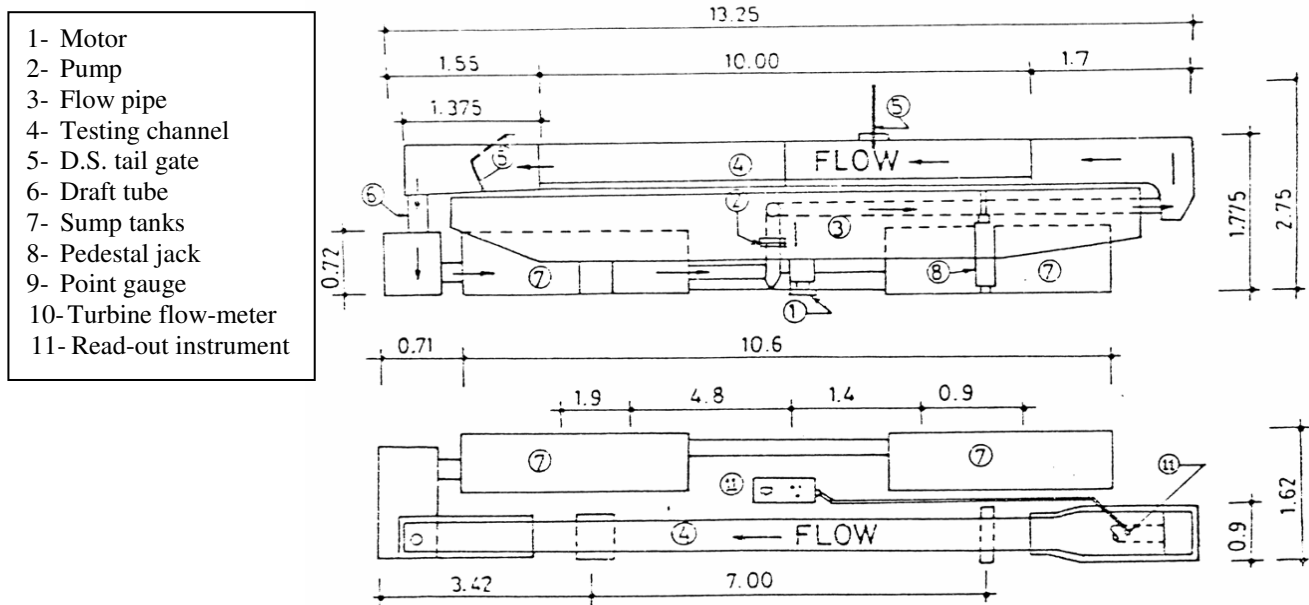


**Fig. (2) A Schematic diagram of the experimental device (flume) used**

**Experimental models:** The experimental works were conducted on four models of sharp-edged V-notch weirs of different V-notch angle ( $\theta$ ) (30°, 60°, 90° and 120°) and for three different Fr (0.0575, 0.0977 and 0.1288). The models are made from steel of

0.45 cm in thickness. The work were repeated at four different weir oblique angles ( $\alpha$ ) (0 (normal weir), 5°, 10° and 15°)

**Test objectives:** The test objectives can be divided into three main categories. The first is to study the effect of changing Fr on the scour downstream models. The second is to investigate the effect of weir angle ( $\theta$ ) while the third test objective is to study the effect of changing the oblique angle ( $\alpha$ ) on the scour and scour configuration pattern.

### **Test procedure**

**Run duration:** at the beginning of the experimental works, some tests of the duration time of runs were conducted for some different weir models with different discharges. The overall time was taken as four hours and the scour depth was recorded every 10 minutes. It was found that at time = 20 minutes the scour depth reach around 75-85% its maximum value at time equal four hours. Consequently, the duration of the run of any test was fixed equal to 20 minutes.

### **Run procedure**

The test procedures were as follows: 1- The weir model was adjusted to the required  $\alpha$  angle and fixed carefully in the flume; 2- At the beginning of each run the sand bed was leveled at the apron level (15 cm in depth); 3- The pump was activated and the discharge was adjusted using a control valve and the reading of the point gauge of the 90 V-notch to give the required discharge; 4- In order to fix the Froude number for each discharge value, the downstream water depth was fixed for each discharge by using the flap tail gate. The run time begin when water touch the downstream apron. 4- After 20 minutes, the pump was stopped and the flume was empties from water by the D.S. tail gate; 5- The sand level was recorded using point gauge through a grid of 5 cm x 5cm until approximately the end of changing of the original bed level (60 cm in case of maximum change); 6- The previous steps were repeated for all the rest of the runs.

## **RESULTS AND DISCUSSION**

Before we go through results and discussion related, it will be more comprehensive if we try to illustrate the different flow patterns for the normal and oblique weirs based on the experimental observation. Next, the section will be divided into three categories; the first one will discuss the effect of changing discharge (Froude number Fr) on the scour parameters while the second will discuss the effect of changing the weir angle ( $\theta$ ). Finally, the third category will discuss the effect of changing the oblique angle ( $\alpha$ ) on the scour parameters.

### **1- Flow pattern downstream normal/oblique weirs**

Figure (3) shows the flow through the normal and oblique weirs based on the experimental observations. For both weir positions the flow lines will be accelerated when they pass over the weir notch. It is clear from the figure that in normal weir,

stream lines of flow move in high speed downstream through a strip at the middle of the flume due to the contraction caused by the weir notch. This high energy of the flow may be the cause of producing maximum scour profile at the middle for the case of normal weir. Directly after the water pass the weir notch to the downstream and due to the contraction of the notch, some vortices and eddies are generated on both sides of the weir and the direction of the flow on the both side of the weir goes towards the adjacent walls W1 and W2, hit them and diverted to the other direction. Both of the walls will be exposed to the same value of disturbance. This disturbance may be the cause of deep scour depth adjacent to the wall.

For the oblique weir, the direction of the stream lines after passing over the notch directed away from the center line of the flume and move towards one of the walls (W1) causing high disturbance in this area. The flow hit the wall and was diverted towards the other direction. On the other hand and for wall W2, some vortex and eddies will be generated and small disturbances will be created but most of such disturbances will be dissipated on the solid bed (apron). This may be the reason of maximizing the scour depth/length for the area adjacent to W1 and creating the overall scour hole near W1. For both weirs and after some distance the flow will be uniform again for all stream lines.

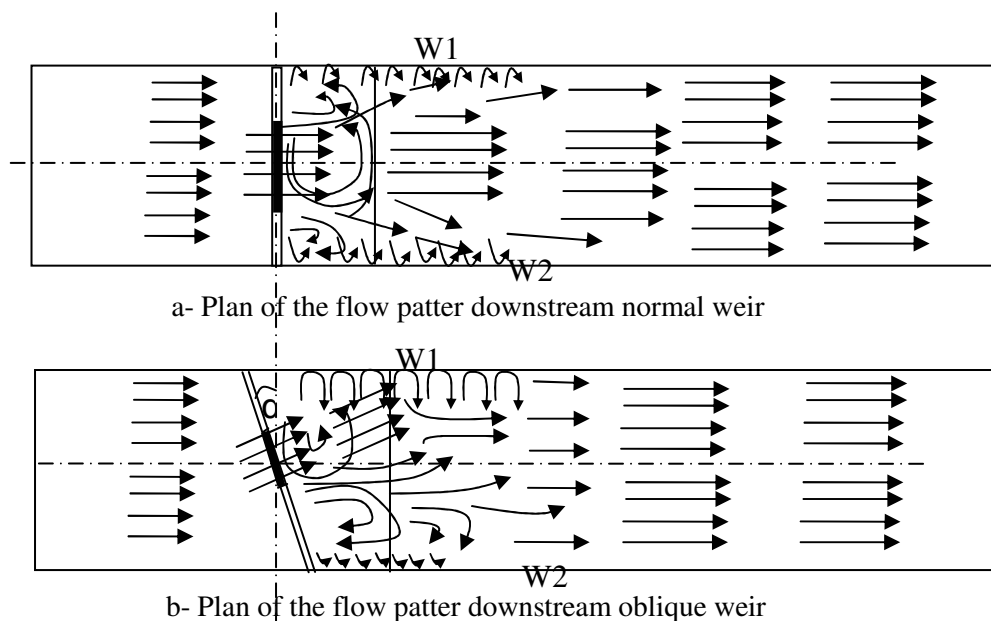


**Fig. (3) Flow pattern downstream the weir models**

## 2- Effect of changing Froude number (Fr) on the scour profile

Figure (4) shows an example for a three dimensional plot for the scour profile for  $\theta = 90^\circ$ ,  $\alpha = 0$  (normal weir) and different Fr values. Figure (5) shows an example of cross sections through the point of maximum scour depth for  $\theta = 90^\circ$ ,  $\alpha = 0$  (normal weir) and different Fr values while Figure (6) shows an example of longitudinal

sections through the center line of the flow for different Fr values. From the figures it is clear that scour parameters increased gradually with the increase of Fr. Point of maximum scour depth appears at the middle area after the apron as a result of high flow velocity coming from the weir notch. Two deep points of scour depth appears adjacent to the walls (W1, W2) which probably resulted from vortex and eddies and disturbance from streamlines hit the walls and diverted to the other direction. It is clear from Figure (4) that the sedimentation height at the center line area is less than that at both sides especially at higher Fr values while the scour length is bigger. This may be due to the higher velocity of the stream lines at the middle part.

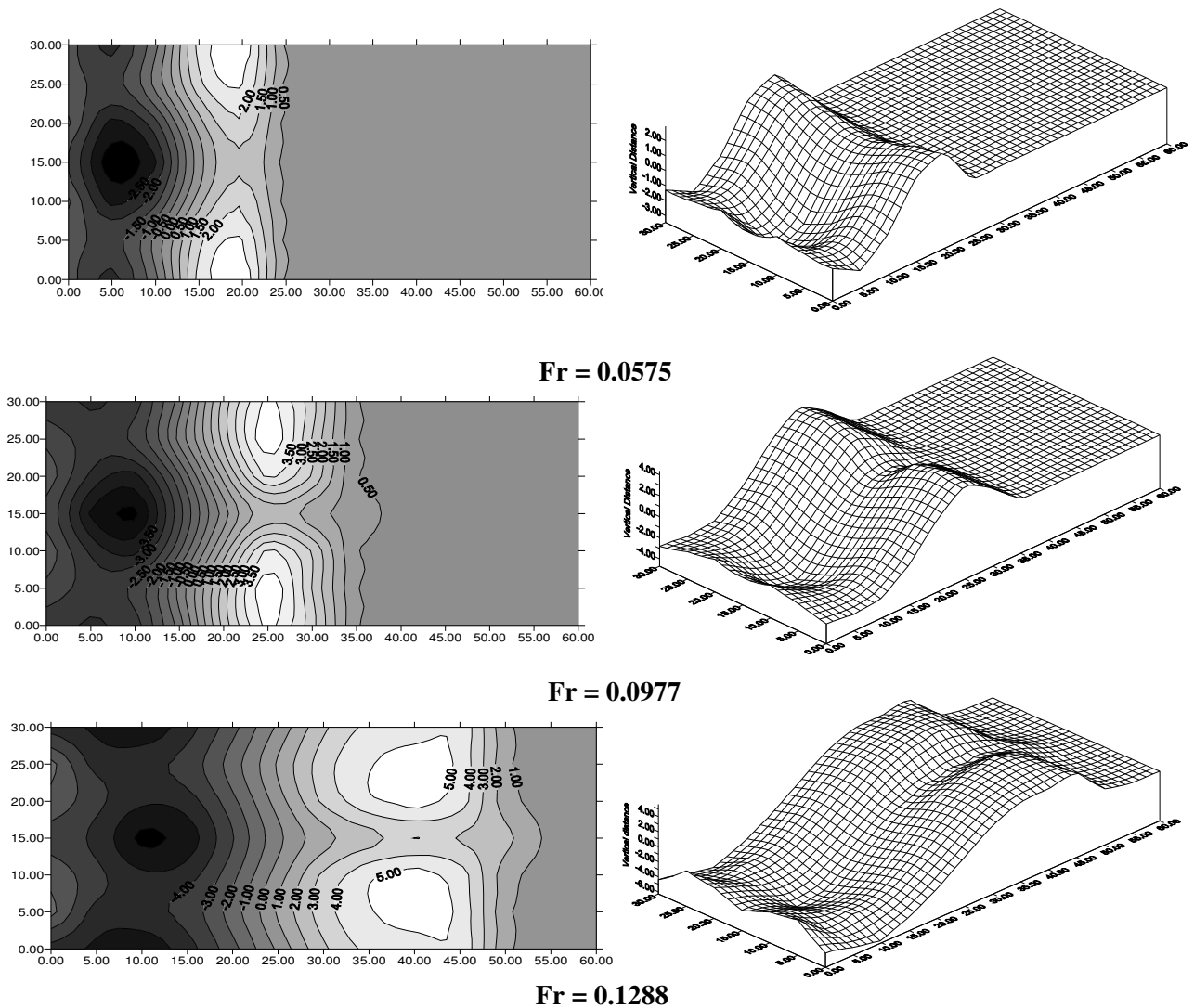


**Fig. (4) Three dimensional plots and contour maps for  $\theta = 90^\circ$ ,  $\alpha = 0$  (normal weir) and different Fr values**

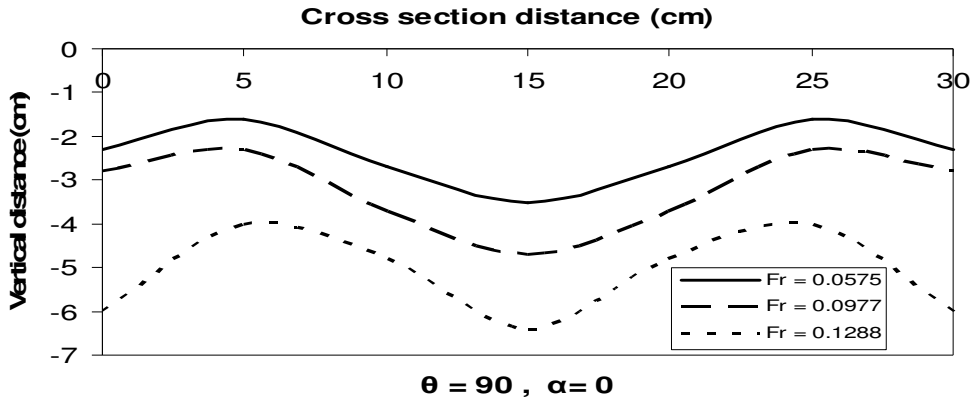


Fig. (5) Cross sections through the point of maximum scour depth for different Fr values ( $\theta = 90^\circ, \alpha = 0$  (normal weir))

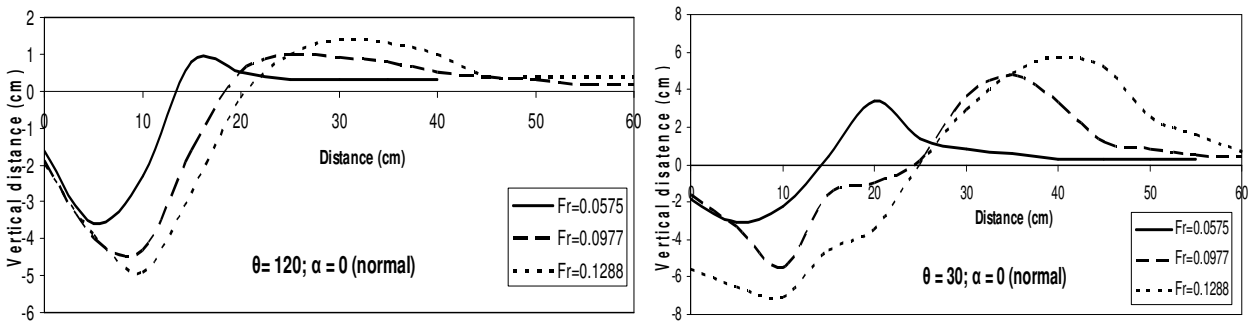


Fig. (6) Longitudinal sections through the center line of the flow for different Fr values ( $\alpha = 0$  (normal weir),  $\theta = 120^\circ, 30^\circ$ )

## 2- Effect of V-notch angle ( $\theta$ ) on the scour profile

Figure (7) shows a three dimensional plots and contour maps for variable values of weir angle ( $\theta$ ) for  $Fr = 0.0575$  and  $\alpha = 0$  (normal weir). Figure (8) shows longitudinal sections through the center line of the flow for different  $\theta$  values ( $\alpha = 0$ , normal weir case) for two different values of Fr. From the figures it can be concluded that scour parameters decrease by the increase of ( $\theta$ ) from  $30^\circ$  to  $60, 90$  and  $120^\circ$ . The overall decrease is not significant between angle  $30, 60$  and  $90^\circ$  and maybe random in some cases while it is too clear if it comes to  $120^\circ$ . It is maybe due to the higher potential energy of the flow in case of smaller angle degree resulted from higher working head (H) for the lower angle. Angle  $120^\circ$  has a minimum potential energy resulted from minimum (H) (4-6cm) while angle  $30^\circ$  has a maximum potential resulted from maximum (H) (10.5-14.5 cm).

Figures (9, 10, 11) show the relationships between weir angle ( $\theta$ ) and  $(ds_{max}/Hd.s)$ ,  $(Ls_{max}/Hd.s)$  and  $(Vs/(Hd.s)^3)$  for different Fr and different values of oblique angle



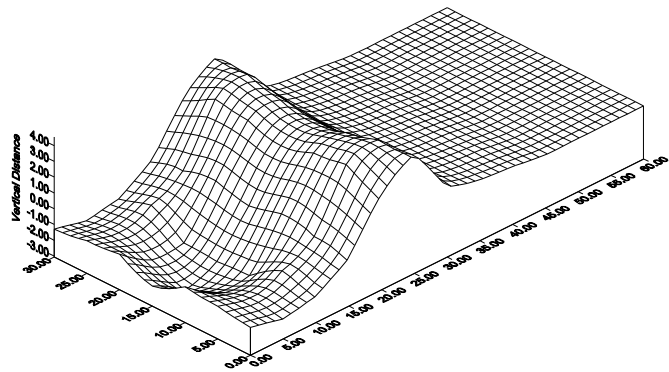
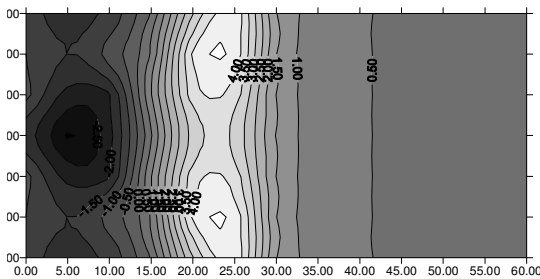
$\alpha$ . Again it is clear that the overall trend is the decrease of the maximum scour parameters with the increase of weir angle from 30, 60, 90 and 120°. The decrease between angles 30, 60 and 90° is not significant and maybe random in some cases. It is maybe due to the small different of working head between the three angles especially between angles 30 and 60°.

The empirical relationships between the weir angle and the maximum scour parameters can be written as follows ( $\theta$  in degrees):

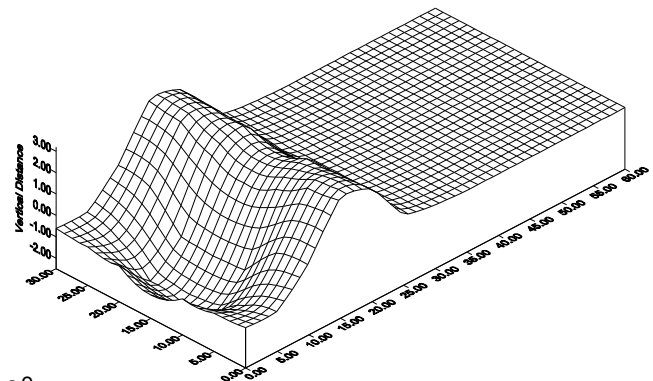
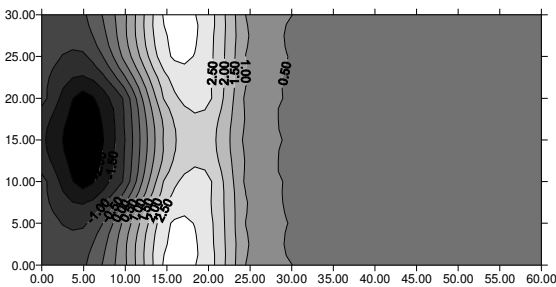
$$ds_{max}/Hd.s = C1 (\theta) + C2 \tag{6}$$

$$Ls_{max}/Hd.s = C3 (\theta) + C4 \tag{7}$$

$$Vs/(Hd.s)^3 = C5 (\theta) + C6 \tag{8}$$



$\theta = 30^\circ$



$\theta = 60^\circ$

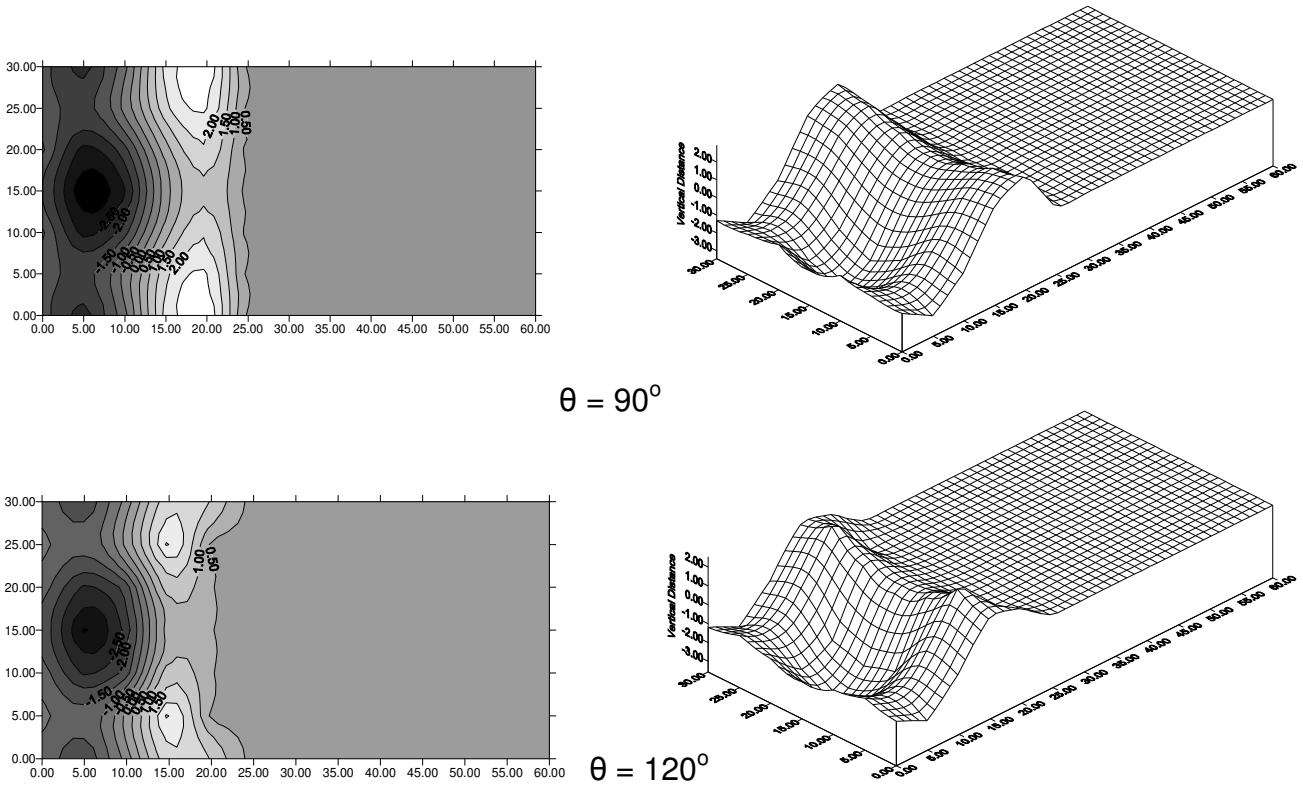


**Fig. (7) Three dimensional plots and contour maps for variable values of weir angle ( $\theta$ ) ( $Fr = 0.0575, \alpha = 0$  (normal weir))**

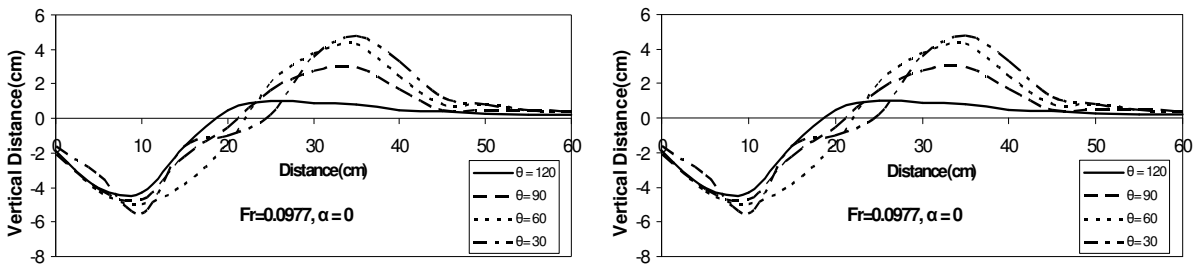


**Fig. (8) Longitudinal sections through the center line of the flow for different  $\theta$  values ( $\alpha = 0$ , normal weir)**

Tables (1) to (3) show values of constants C1 to C6 in Equations (6-8) for Figures (9-11).

**Table (1) values of C1, C2 in equation (6)**

Scour parameters	Fr	Oblique angle	C1	C2	Oblique angle	C1	C2
dsmax	0.0575	$\alpha = 5$	-0.0008	0.4625	$\alpha = 15$	-0.0017	0.6644
	0.0977		-0.0009	0.5312		-0.001	0.7319
	0.1288		-0.0021	0.7325		-0.0022	1.0576

**Table (2) values of C3, C4 in equation (7)**

Scour parameters	Fr	Oblique angle	C3	C4	Oblique angle	C3	C4
Lsmax	0.0575	$\alpha = 10$	-0.0047	2.0821	$\alpha = 0$	-0.0076	2.9643
	0.0977		-0.0038	2.8845		-0.011	4.1449
	0.1288		-0.0084	3.6666		-0.0134	4.75

**Table (3) values of C5, C6 in equation (8)**

Scour parameters	Fr	Oblique angle	C5	C6	Oblique angle	C5	C6
Vs	0.0575	$\alpha = 5$	-0.005	1.6737	$\alpha = 0$	-0.0029	1.6222
	0.0977		-0.0125	3.0489		-0.0064	3.1483
	0.1288		-0.0222	4.7417		-0.029	6.2857

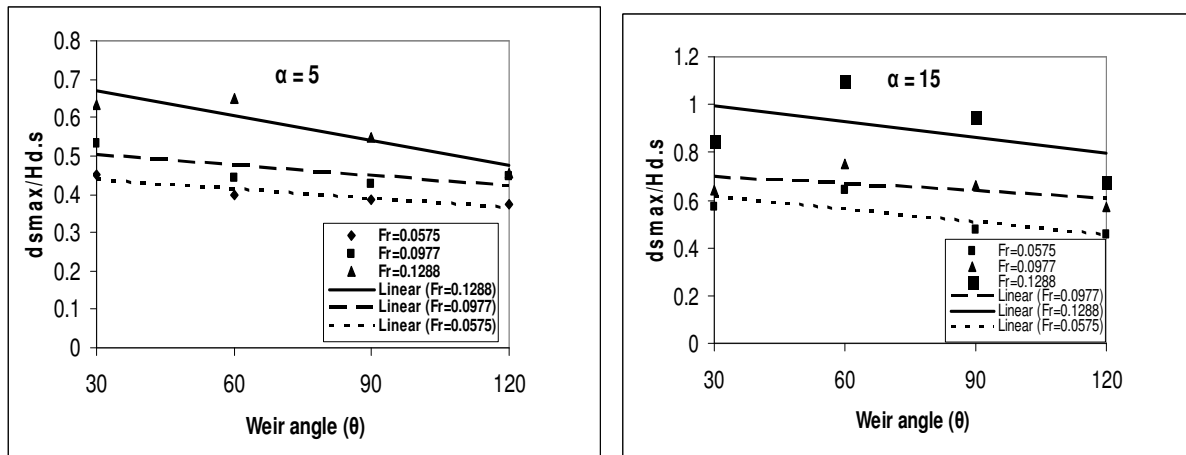


**Fig. (9) The relationship between Weir angle ( $\theta$ ) and ( $ds_{max}/Hd.s$ ) for different Fr values ( $\alpha = 5, 15$ )**

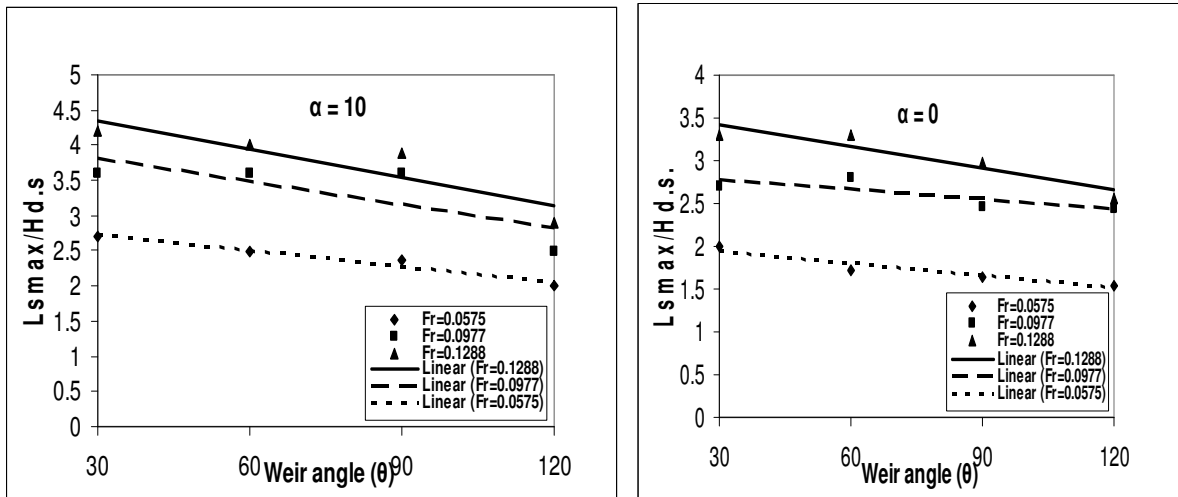


Fig. (10) The relationship between Weir angle ( $\theta$ ) and ( $Ls_{max}/Hd.s$ ) for different Fr values ( $\alpha = 10, 0$ )

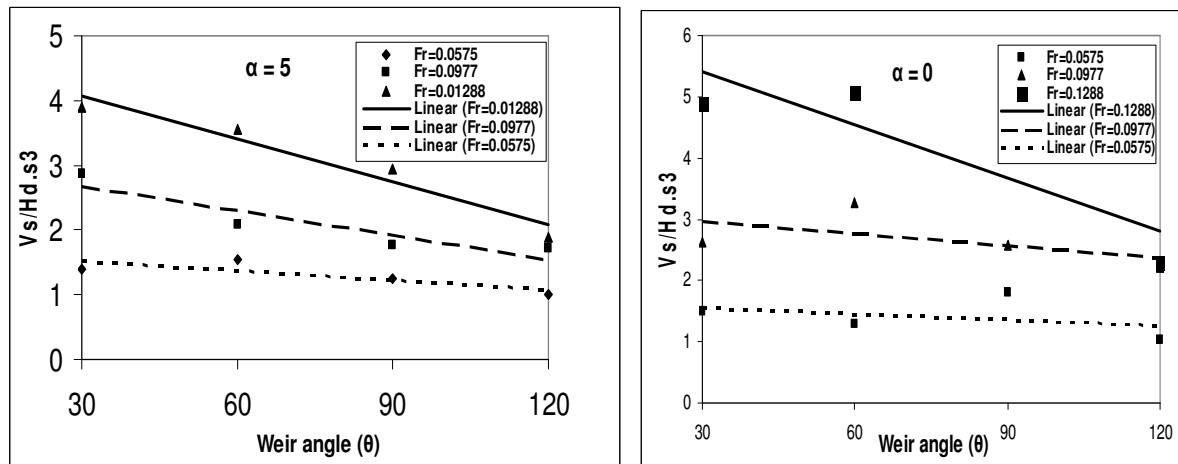
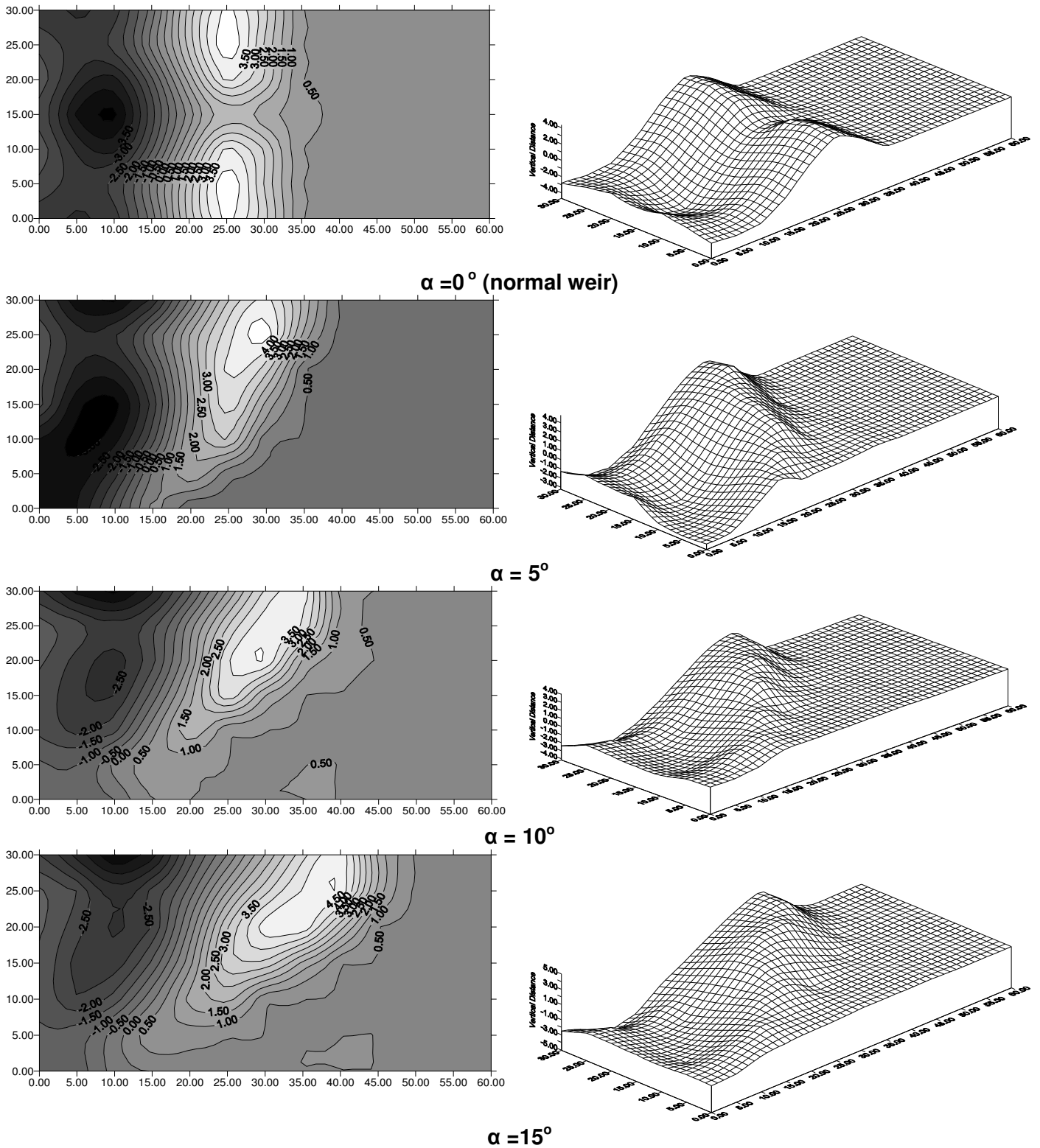


Fig. (11) The relationship between Weir angle ( $\theta$ ) and ( $Vs/(Hd.s)^3$ ) for different Fr values ( $\alpha = 5, 0$ )

### 3- Effect of oblique angle ( $\alpha$ ) on the scour profile

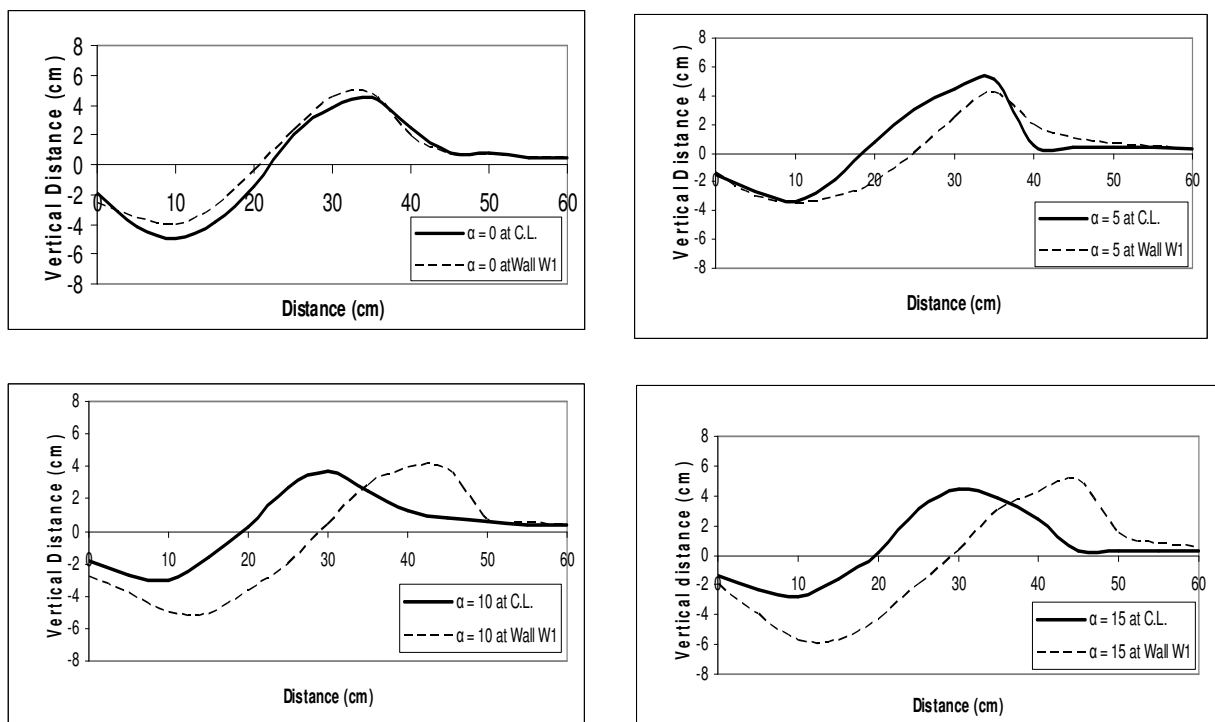
When the V-notch weir rotates by angle ( $\alpha$ ) in the horizontal plan, it directs the flow towards one of the walls (W1) (see Figure (3)). Consequently, the shape of the scour hole will be changed. Figure (12) shows an example of three dimensional plots and contour maps for the scour hole profile for weir angle  $\theta = 90^\circ$  and  $Fr = 0.0977$  and different values of the oblique angle ( $\alpha$ ). It is clear from the figure that scour hole is formed at the middle part in the case of normal weir. By increasing angle ( $\alpha$ ), the scour hole moves gradually towards wall W1.



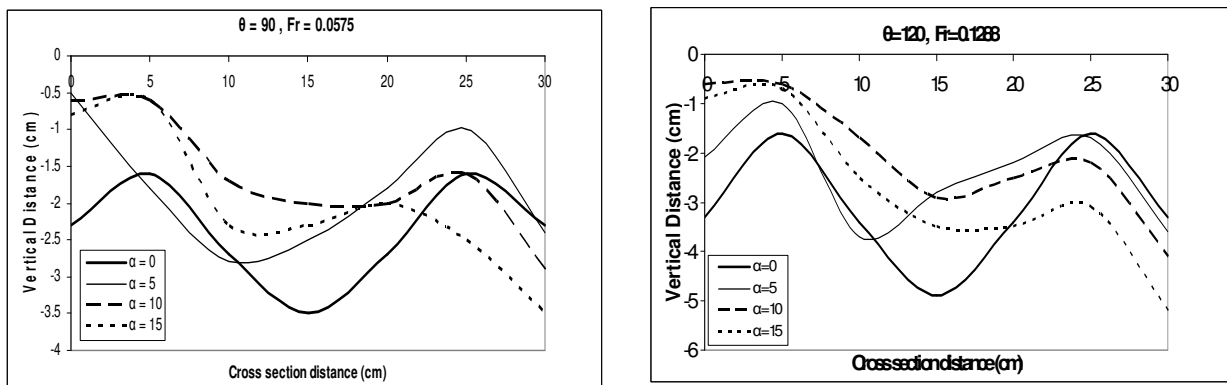
**Fig. (12) Three dimensional plots and contour maps for weir angle  $\theta = 90^\circ$  and  $Fr = 0.0977$  and different values of the oblique angle ( $\alpha$ )**

Figure (13) shows examples of comparison between longitudinal section at the center line and section adjacent to wall W1 for different values of oblique angle ( $\alpha$ ) while Figure (14) shows examples for cross sections through the point of maximum scour

depth for different  $\alpha$  values . From the figures it is clear that scour parameters ( $d_s$ ,  $L_s$ ) values at section adjacent to the wall W1 are slightly less than those of the section at the center line for the normal weir case. By increasing angle ( $\alpha$ ), scour parameters ( $d_s$ ,  $L_s$ ) adjacent to the wall W1 increase dramatically especially at higher values of ( $\alpha$ ) ( $10^\circ$ ,  $15^\circ$ ). On the other hand, the scour parameters decrease at the middle part. The reason for these changes may be explained by the following; in oblique weir, the velocity of flow passing the end of the apron is less than that of normal weir and consequently, it results less scour depth/length values at the middle part than that of normal weir. On the other hand, due to the oblique weir location, flow lines are approaching the wall W1 causing higher disturbance (backward movement of the flow when it hits the wall) than that of normal weir resulting deeper scour depth/length adjacent to W1.



**Fig. (13) Comparison between longitudinal section at the center line and adjacent to wall W1 for different values of oblique angle ( $\alpha$ ) ( $\theta = 60^\circ$ ,  $Fr = 0.0977$ )**



**Fig. (14) Cross sections through the point of maximum scour depth for different  $\alpha$  values ( $\theta = 90^\circ$ ,  $120^\circ$ )**

Figure (15) shows examples of the relationship between oblique angle ( $\alpha$ ) and ( $d_{smax}/Hd.s$ ) for different Fr values. The range of the angle ( $\alpha$ ) is between 0 and 15°. It is clear from the figure that maximum scour depth decreases for small oblique angle (0-5°). By increasing oblique angle from 5° to 15°,  $d_{smax}$  starts to increase again. It can be justified by the following; at small oblique angles the flow lines don't approaching enough to the Wall W1 in order to increase the scour depth adjacent to the wall significantly. On the other hand and due to smaller velocity of the flow lines than of the normal weir, the maximum scour in case of the normal weir at the middle part decreases producing the overall maximum scour depth in case of small oblique angle to be less that of a normal weir. By increasing the oblique angle, the flow line approaching enough to the wall to cause a deeper scour depth more than that of normal weir.

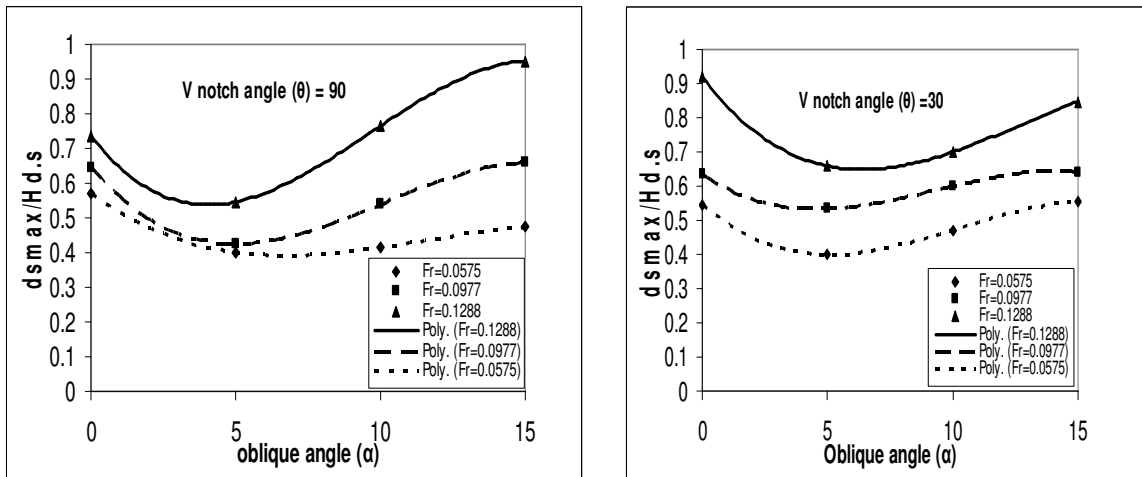


**Fig. (15) The relationship between oblique angle ( $\alpha$ ) and ( $d_{smax}/Hd.s$ ) for different Fr values ( $\theta = 30^\circ, 90^\circ$ )**

Figure (16) shows examples of the relationship between oblique angle ( $\alpha$ ) and ( $L_{smax}/Hd.s$ ) for different Fr values. As a general trend, maximum scour length  $L_{smax}$  increases by the increasing of the oblique angle ( $\alpha$ ) for the same reason explained before. The position of the maximum scour length is adjacent to wall W1. Figure (17) shows examples of the relationship between oblique angle ( $\alpha$ ) and ( $V_s/(Hd.s)^3$ ) for different Fr values. By the increasing of angle ( $\alpha$ ) the scour hole moves towards the wall W1 resulting a decrease of its volume. For higher values of angle ( $\alpha$ ) the scour depth increased dramatically and may cause the volume of scour hole to increase again.

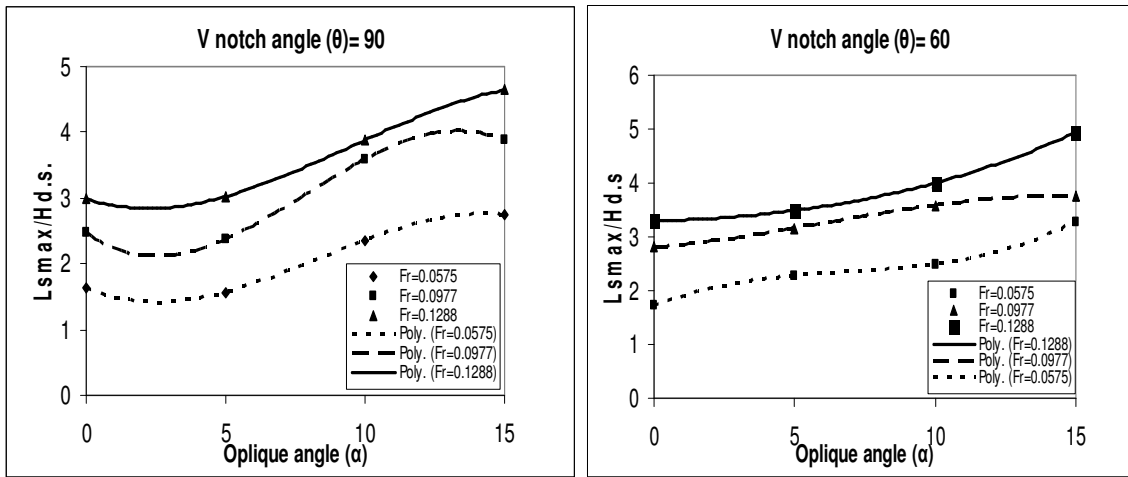


Fig. (16) The relationship between oblique angle (α) and (Lsmax/Hd.s) for different Fr values (θ = 60°, 90°)

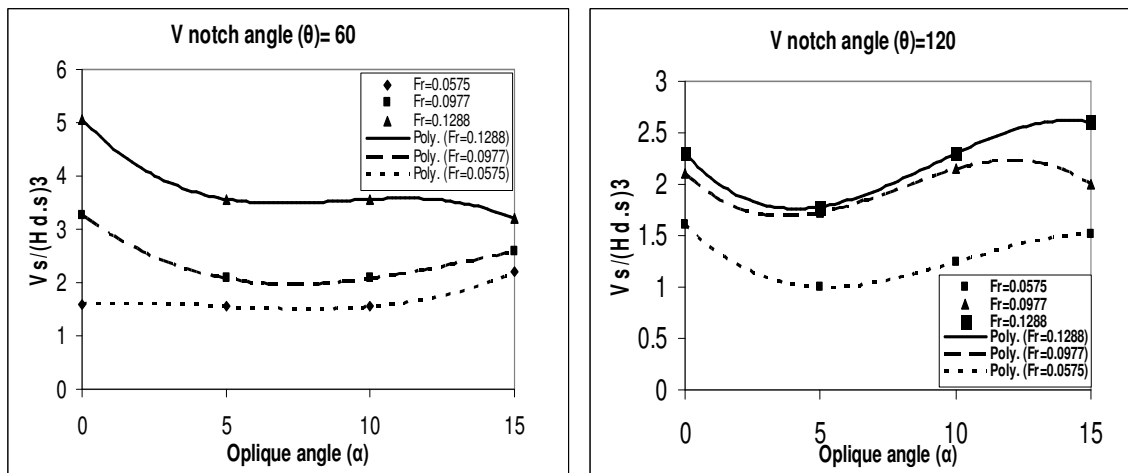


Fig. (17) The relationship between oblique angle (α) and (Vs/(Hd.s)³) for different Fr values (θ = 60°, 120°)

The empirical relationships between the oblique angle (α) and the maximum scour parameters can be written as follows (α in degrees):

$$ds_{max}/Hd.s = C1 (\alpha)^3 + C2 (\alpha)^2 + C3 (\alpha) + C4 \tag{9}$$

$$Ls_{max}/Hd.s = C5 (\alpha)^3 + C6 (\alpha)^2 + C7 (\alpha) + C8 \tag{10}$$

$$Vs/(Hd.s)^3 = C9 (\alpha)^3 + C10 (\alpha)^2 + C11 (\alpha) + C12 \tag{11}$$

where, (α = 0-15°)

Tables 4, 5 and 6 show values of constants C1 to C12 in Equations 9, 10 and 11 for the Figures (15) to (17).



**Table (4) values of C1 – C4 in equation (9)**

Scour parameters	Fr	Weir angle	C1	C2	C3	C4
dsmax	0.0575	$\theta = 90$	-0.0002	0.0065	- 0.0623	0.5714
		$\theta = 30$	-0.0003	0.0085	- 0.0648	0.5467
	0.0977	$\theta = 90$	-0.0004	0.0132	- 0.0994	0.6456
		$\theta = 30$	-0.0003	0.0072	- 0.0498	0.6341
	0.1288	$\theta = 90$	-0.0006	0.0169	- 0.1077	0.7356
		$\theta = 30$	-0.0003	0.0099	- 0.0947	0.9176

**Table (5) values of C5 – C8 in equation (10)**

Scour parameters	Fr	Weir angle	C5	C6	C7	C8
Lsmax	0.0575	$\theta = 90$	-0.0017	0.0421	- 0.1833	1.6429
		$\theta = 60$	0.0012	- 0.025	0.2118	1.7143
	0.0977	$\theta = 90$	-0.0030	0.0708	- 0.2983	2.4684
		$\theta = 60$	-0.0004	0.0076	0.0444	2.8049
	0.1288	$\theta = 90$	-0.0012	0.0349	- 0.137	2.9885
		$\theta = 60$	0.0001	0.0041	0.0145	3.2941

**Table (6) values of C9 – C12 in equation (11)**

Scour parameters	Fr	Weir angle	C9	C10	C11	C12
Vs	0.0575	$\theta = 60$	0.0008	- 0.0109	0.025	1.6
		$\theta = 120$	-0.0011	0.0327	- 0.256	1.6
	0.0977	$\theta = 60$	-0.0009	0.0378	- 0.4046	3.271
		$\theta = 120$	-0.0018	0.0433	- 0.2458	2.1
	0.1288	$\theta = 60$	-0.0025	0.0675	- 0.5762	5.069
		$\theta = 120$	-0.0017	0.0459	- 0.2918	2.3

## SUMMARY AND CONCLUSIONS

Laboratory experiments were conducted in order to investigate the effect of oblique V-notch weir on the scour profile downstream the weir. Four weir models of different V-notch angles (30, 60, 90 and 120°) were tested. Weirs were adjusted at four positions of oblique angle (0, 5, 10 and 15°). Three different discharges were used. The main objective of the study is to investigate whether using oblique weir will contribute for decreasing the scour downstream the weir or it will increase the problem. Moreover, the study tested the effect of changing the V-notch weir angle on the scour profile. Effect of changing discharge also has been investigated.

Results showed that the effect of changing the V-notch weir angle on the scour profile is not significant for the first three weir angles (30, 60 and 90°). On the other hand, the maximum scour parameters (maximum scour depth, maximum length of scour and volume of scour) have decreased significantly if the weir angle is changed to 120°. Results showed also that scour parameters were increased with the increase of discharge.

Results revealed that by positioning the V-notch weir with small oblique angle in the horizontal plane (up to 5°), both the maximum scour depth and volume of scour were decreased in all weirs models with different V-notch angles. Both the maximum scour depth and maximum scour length started to be increased again when the oblique angle was increased up to 15°. Point of maximum scour appeared at the center line for the normal weir and started to move gradually towards the wall located in direction of the flow with small oblique angle. By increasing the oblique angle, point of maximum scour became adjacent to the wall located in direction of the flow. Based on some trials which were not shown in the present study, by increasing the oblique angle more than 15°, the flow lines approached the wall very closely and with bigger angle, they hit the wall above the apron which threatens the stability of the weir walls at the real field. Empirical equations defining maximum scour depth/length and volume of scour hole with different variables were developed.

It was concluded that using small oblique weir angle in the horizontal plan, scour risk downstream weir could be minimized.

## **ACKNOWLEDGMENTS**

The authors want to express their gratitude to Prof. Shaaban Abdou, Dean of Faculty of Engineering, Suez Canal University for his great assistance and kind help. Special thanks to Prof. Mohamed Balah, Civil Engineering Department, Faculty of Engineering, for his useful suggestions and helpful advices.

## **REFERENCES**

- 1- Abo-Zeid, G.A., 2004, "Scour at the abutments of one-vent bridges", *J. of Eng. Science (JES)*, Assiut University, Vol. 32, No. 3, July 2004.
- 2- Abo-Zeid, G.A., 2006, "Estimation of the minimum floor length behind sluice gates against scour utilizing solid bed and erodible basin", *J. of Eng. Science (JES)*, Assiut University, Vol. 34, No. 4, July 2006.
- 3- Ali, N.A., 1995, "The proper location of floor sill with scour reach downstream of heading-up structure", *J. of Eng. Scie. (JES)*, Faculty of Engineering, Assiut University, 23(2), July 1995.
- 4- Ali, N.A., 1996, "Scour prediction at submarine pipelined near the sea bed", *Bulletin of Faculty of Engineering, Assiut University*, 24(1), Jan. 1996.

- 5- Ashour, M.A., Bestawy, A.M., and Ali, K.A., 2003, "Optimization of row numbers of baffles downstream heading-up structures for reducing scour hole", 1<sup>st</sup> International Conference of Civil Engineering Science, ICCESI, Vol. 2, 2003, pp. 82-88.
- 6- Borghei, S.M., Vatannia, Z., Ghodsian, M., Jalili, M. R., 2003, "Oblique rectangular sharp-crested weir", *Water & Maritime Engineering* 156, Issue WM2, pp. 185-191.
- 7- Hassan, M.K. and Narayanan, R., 1986, "Local scour downstream of an apron", *Journal of Hydraulic Engineering*, Vol. 111, No. 11, November, pp. 1371-1385.
- 8- Hemaid, H.S., 2000, "Bed erosion at submarine pipelines exposed to unidirectional water flow", M.Sc. Thesis, Civil Eng. Dept., Assiut University, Egypt.
- 9- Kamil, H. M., and Karim O. 2002, "Simulation of flow around piers", *J. of Hydr. Res. (IAHR)*, 40(2).
- 10- Nasr and Nagy, 1997, "Local scour and riprap protection downstream water spillways", *Alexandria Eng. J.*, Vol. 36, No. 6.
- 11- Negm, A.M., Abdel-Aal, G.M., Saleh, O.K., and Saudia, M.F., 2002, "Effect of subcritical flow on scour characteristics downstream of sudden expansion stilling basins", *Egyptian Journal for Engineering Science and Technology EJEST*, Vol. 6, No 1, pp. 1-13.
- 12- Prakash, M.N.S. and Shivapur A. V., 2004, "Flow over Sharp-crested inclined Inverted V-notch weir", *Journal of Irrigation and Drainage Engineering*, Vol. 130, No. 4, August 2004.
- 13- Roudkivi, A.J., and Ettema, R. 1983, "Clear-water scour at cylindrical piers", *Journal of Hydraulic Engineering*, 109(3), pp. 338-350.
- 14- Tuyen, N. B., 2006, Flow over oblique weirs. A master thesis, Civil Engineering and Geosciences Department, Delft University of Technology.
- 15- Yousef, H., 2004, "A new analytical bridge pier scour equation", *Proc. of 8<sup>th</sup> Int. Water Technology Conference (IWTC)*, Alexandria, Egypt.

## NOMENCLATURE

ds	Scour depth,
dsmax	Maximum scour depth,
d <sub>50</sub>	Mean particle diameter of bed material,
Fr	Downstream Froude number,
H	Working head of the weir,
Hd.s	Downstream water depth,
g	Acceleration of the gravity,
L	Length of apron,
Ls	Length of Scour hole,
Lsmax	maximum scour length,
Re	Reynolds number,
Q	Water discharge through the flume,
t	Time of the run,

$V$	Normal mean velocity at the downstream cross section of the channel,
$V_s$	Volume of the scour hole,
$\theta$	V-notch angle,
$\alpha$	Oblique angle of the weir,
$\gamma_w$	Specific weight of water,
$\gamma_s$	Soil particle specific weight, and
$\nu$	Kinematic viscosity.